

## High performance of ZnO nanowire protein sensors enhanced by the piezotronic effect

Cite this: DOI: 10.1039/c2ee23718k

Ruomeng Yu,<sup>†a</sup> Caofeng Pant<sup>ab</sup> and Zhong Lin Wang<sup>\*ab</sup>

Received 7th October 2012

Accepted 18th December 2012

DOI: 10.1039/c2ee23718k

[www.rsc.org/ees](http://www.rsc.org/ees)

Based on a metal–semiconductor–metal structure, the performance of a ZnO nanowire (NW) based sensor has been studied for detecting Immunoglobulin G (IgG)-targeted protein. By applying a compressive strain, the piezotronic effect on ZnO NW protein sensors can not only increase the resolution of such sensors by tens of times, but also largely improve the detection limit and sensitivity. A theoretical model is proposed to explain the observed behaviors of the sensor. This study demonstrates a prospective approach to raise the resolution, improve the detection limit and enhance the general performance of a biosensor.

Sensitive, selective, and cost-effective detection of biomolecules has huge applications in clinical diagnostics, industrial and environmental monitoring.<sup>1–3</sup> Semiconducting nanowire (NW) based field effect transistors (FETs) are one of the candidates for biosensing<sup>4–7</sup> that have large surface areas and can be easily functionalized for various bio-detection.<sup>8–11</sup> Wurtzite and zinc blend structured semiconductors, such as ZnO, GaN, CdS and CdSe, usually exhibit the piezoelectric effect. Strain induced piezoelectric polarization inside these materials can be used to tune the transport properties of such semiconductor NW-based devices, which is known as the piezotronic effect.<sup>12</sup> Piezotronics is about the devices fabricated using the piezopotential as a “gate voltage” to tune/control charge transport across an interface or junction.<sup>13</sup> Therefore, the performance of ZnO NWs can be tuned by the piezotronic effect for high performance strain sensors,<sup>14</sup> UV sensors,<sup>15</sup> photodetectors,<sup>16</sup> and LEDs.<sup>17</sup>

In this work, we study the piezotronic effect on the performance of a ZnO NW-based protein sensor by using a metal–semiconductor–metal (MSM) structured Schottky contacted

### Broader context

Sensitive, selective, and cost-effective detection of biomolecules has huge applications in clinical diagnostics, industrial and environmental monitoring. Semiconducting nanowire (NW) based field effect transistors (FETs) are one of the candidates for biosensing and various bio-detection. In this work, the performance of a ZnO NW based sensor has been studied for detecting Immunoglobulin G (IgG)-targeted protein. By applying a compressive strain, the piezotronic effect on ZnO NW protein sensors can not only increase the resolution of such sensors by tens of times, but also largely improve the detection limit and sensitivity. A theoretical model is proposed to explain the observed behaviors of the sensor. This study demonstrates a prospective approach to raise the resolution, improve the detection limit and enhance the general performance of a biosensor.

device. ZnO NW devices functionalized with gold nanoparticle–anti-Immunoglobulin G conjugates (Au NP–anti-IgG) can respond to a specific kind of protein Immunoglobulin G (IgG) as a protein sensor.<sup>18</sup> The adsorption of IgG, which is positively charged, is equivalent to adding a positive potential gating that leads to an increased electron density within an n-type ZnO NW-based FET.<sup>19,20</sup> That is, for a strain free ZnO NW sensor, the higher the IgG concentration, the higher the output signal of the ZnO NW device. When a strain was applied on the ZnO NW sensor, it produced a piezopotential in the ZnO NW along the *c*-axis, which tuned the effective height of the Schottky barrier at local contacts, and then influenced the output signals of the device. In this paper, we systematically studied the piezotronic effect on the performance of a ZnO NW based protein sensor by carrying out the performance tests of the sensor under different externally applied strains and different IgG concentrations. Our results show that the piezotronic effect on ZnO NW protein sensors can raise the resolution of such protein sensors by tens of times and largely improve the detection limit and sensitivity of ZnO NW protein sensors by introducing a compressive strain. A model using energy band diagrams is proposed to explain the observed behaviors. This study demonstrates a prospective approach to raise the resolution, improve the detection limit and enhance the general performance of biosensors.

<sup>a</sup>School of Materials Science and Engineering, Georgia Institute of Technology, Atlanta, Georgia 30332-0245, USA. E-mail: [zlwang@gatech.edu](mailto:zlwang@gatech.edu); Web: <http://www.nanoscience.gatech.edu>

<sup>b</sup>Beijing Institute of Nanoenergy and Nanosystems, Chinese Academy of Sciences, Beijing, China

<sup>†</sup> These authors contributed equally.

ZnO NWs used in this experiment were synthesized *via* a high temperature thermal evaporation process,<sup>14,21,22</sup> with a length of several hundreds of micrometers and a diameter ranging from tens of nanometers to a few micrometers. The device was fabricated by transferring and binding an individual ZnO NW laterally onto a polyethylene terephthalate (PET)/or a polystyrene (PS) substrate, with its *c*-axis in the plane of the substrate pointing to the source. Silver paste was used to fix the two ends of the NW, serving as source and drain electrodes as well, respectively. This Ag-ZnO NW-Ag device could be treated as a metal-semiconductor-metal (M-S-M) structure.<sup>14</sup> A thin layer of epoxy was used to fully cover both end-electrodes in order to rule out possible contacting between electrodes and the solution when the device is immersed into protein solution. Then gold nanoparticle-anti-Immunoglobulin G conjugates (Au NP-anti-IgG) were assembled onto the surface of ZnO NW by adding 0.01 ml of Au NP-anti-IgG colloidal solution (purchased from Tedpella, used directly without further purification) on the NW and incubated for one hour in a fume hood. Before carrying out the protein Immunoglobulin G (IgG) test, the devices were modified with a blocking buffer (BB) (0.1% Tween 20 (purchased from Tedpella), 0.1% fish gelatin (purchased from Tedpella), and 1% BSA (purchased from Sigma-Aldrich)). It was reported that BB could efficiently block the nonspecific binding of IgGs to the devices.<sup>20</sup> Thus, treating the device with BB can effectively diminish the undesirable response from the nonspecific binding to the device and is necessary for the specific function of the sensor. Devices with BB were dried for two hours at room temperature and then washed with PBS buffer. After that, 0.005 ml of IgG (purchased from Sigma-Aldrich) sample with a given concentration was pipetted onto the device for protein binding for one hour, followed by washing and drying. A schematic in Fig. 1c shows the principle of a strain free and Au NP-anti-IgG decorated ZnO NW protein sensor, with the target protein IgG bonded. The same device applied by external compressive strains is presented in Fig. 1d.

The response of the ZnO NW protein sensor to different IgG concentrations, measured at a fixed bias of 2 V, is presented in Fig. 1e. The response signal of the device (*i.e.* current here) increased significantly from the nA scale to several mA with the increase of the target protein IgG concentrations from 0 to  $1 \times 10^{-3} \text{ g ml}^{-1}$ , since more target protein IgG were adsorbed onto the surface of the ZnO NW. This result indicates that the anti-IgG decorated ZnO NW device has a good response to IgG concentrations. Further detailed examinations were carried out by measuring the current-voltage (*I-V*) curves of the sensor, with a bias voltage ranging from -2 to 2 V. *I-V* curves of a ZnO NW device under different IgG concentrations are presented in Fig. 1f, which indicates that the output signals of the device are much stronger at higher IgG concentrations.

The piezotronic effect on the performance of these ZnO NW sensors was examined when the ZnO NW device was compressively strained. The compressive strain can be calculated according to Yang *et al.*'s work.<sup>23</sup> A three-dimensional (3D) mechanical stage with a movement resolution of 1  $\mu\text{m}$  was used to apply a strain on the free end of the PS substrate, with the other end fixed tightly on a manipulation holder. Fig. 2

shows four sets of *I-V* curves corresponding to different IgG concentrations, which were measured when the ZnO NW device was applied an external compressive strain. The insets in Fig. 2 are corresponding schematic diagrams of the ZnO NW device under different strains and IgG concentrations. Take Fig. 2a as an example to illustrate how the piezotronic effect tuned the performance of ZnO NW protein sensors. The current increases obviously, and the shape of *I-V* curves changes from an "Ohmic type" to a "Schottky type" when the externally applied strain increased from 0%, -0.41%, -0.58%, -0.67%, -0.75% to -0.82%.<sup>23</sup> Similar trends are observed for all the other three sets of *I-V* curves. It is necessary to notice that the variation of the *I-V* curves of ZnO biosensors was attributed to a combination of bulk resistance change (piezoresistance effect) and the piezotronic effect, as reported in previous work.<sup>24</sup> In our case, the piezoresistance effect is a symmetric effect regardless of the sign of the applied bias, hence it increased the output currents at both +2 V and -2 V. On the other hand, the piezotronic effect increased the output current at +2 V, while decreased that at -2 V, because it has a polarity depending on the sign of the local piezoelectric charges. Both effects co-exist in the *I-V* measurements. The *I-V* curves shown in Fig. 2 were derived under the influence of both the piezotronic effect and the piezoresistance effect, but the dominant one is the piezotronic effect.<sup>25,26</sup> Therefore, the *I-V* curves here are not similar to that of a standard diode, but the relative change of currents at +2 V is larger than that at -2 V, because the effective barrier height was decreased without subtracting off the contribution made by the piezoresistance effect. The change in transport characteristics indicates that the piezotronic effect in ZnO NW tunes the effective height of the Schottky barrier at local contacts, which played a very important role in tuning the performance of protein sensors. The non-linear effect introduced by the piezotronic effect in current transport can significantly enhance the sensitivity of the sensor.

By systematically investigating the sensor response to the changing external strain and target protein concentration, the results were extracted and plotted in a 3-dimensional (3D) graph, as shown in Fig. 3a. An overall trend of how output signals vary with the change of IgG concentrations and compressive strains can be simultaneously derived from this 3D graph. It is straightforward to see that the current increases as the IgG concentration or compressive strain increases. Four 2D graphs are shown in Fig. 3b-e for more details and information, which are extracted from Fig. 3a by projecting on the *I-strain* surface and the *I-IgG* concentration surface, respectively.

Fig. 3b and c show the absolute and relative current response of the ZnO NW protein sensor under different compressive strains when the concentration of the target protein was fixed at 0,  $1 \times 10^{-7}$ ,  $1 \times 10^{-6}$  and  $1 \times 10^{-5} \text{ g ml}^{-1}$ , respectively. These 2D graphs present four curves at four IgG concentrations, each was derived by measuring the output current of the ZnO NW protein sensor under different compressive strains. For each curve, it is clear that the output signals increase with the increase in compressive strain, which is in accordance with the previous conclusion: the piezotronic effect can enhance the performance of protein sensors at different IgG concentrations. In addition,

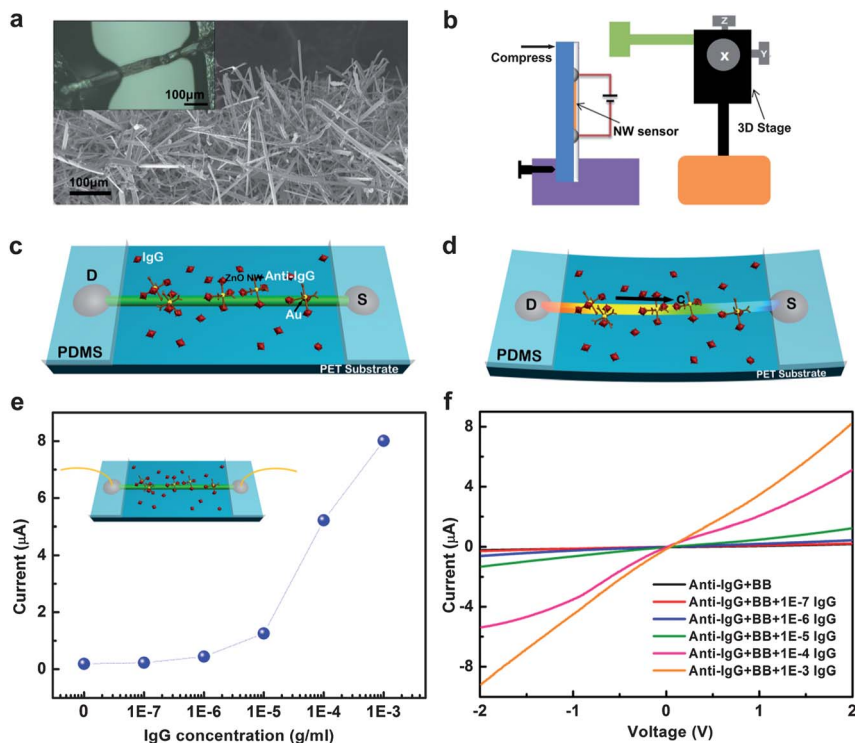


**Fig. 1** Schematic and target protein IgG response of a ZnO NW sensor. (a) SEM image of as-fabricated ZnO NWs. The inset shows an optical microscopy image of a typical ZnO NW sensor. (b) Schematic representation of the ZnO NW device set-up. (c) Gold nanoparticle-anti-IgG surface functionalized ZnO NW protein sensor binding with the target protein IgG. (d) ZnO NW protein sensor under compressive strain. (e) Target protein IgG response of ZnO NW devices at a fixed voltage of 2 V, with the IgG concentration varying from 0 to  $1 \times 10^{-3} \text{ g ml}^{-1}$ , no external strain was applied. (f)  $I$ - $V$  curves of ZnO NW devices at different IgG concentrations, no external strain was applied.

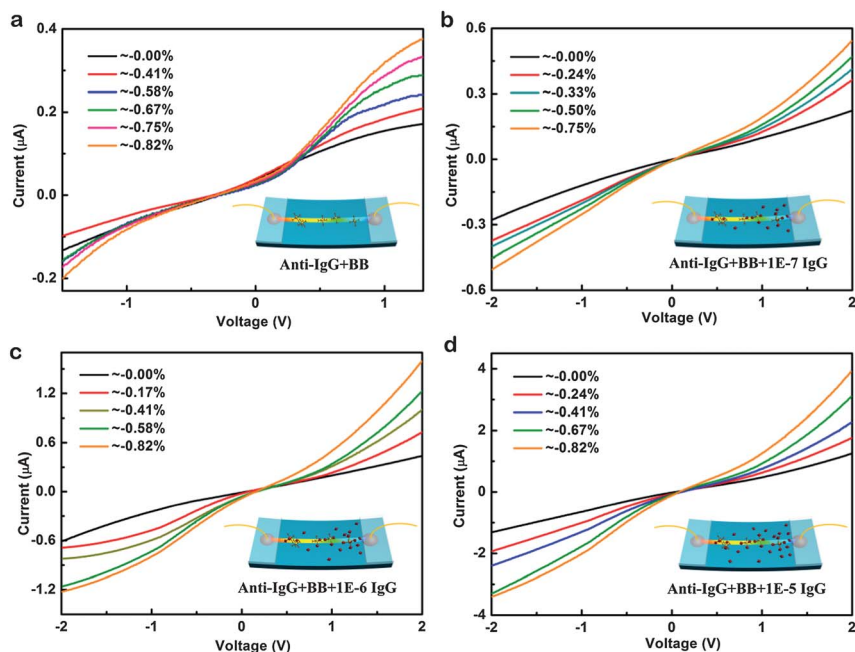


**Fig. 2**  $I$ - $V$  curves of the ZnO NW protein sensor under different degrees of compressive strain, when the device was decorated with (a) anti-IgG and BB, (b) anti-IgG and BB binding with  $1 \times 10^{-7} \text{ g ml}^{-1}$  target protein IgG, (c) anti-IgG and BB binding with  $1 \times 10^{-6} \text{ g ml}^{-1}$  target protein IgG, and (d) anti-IgG and BB binding with  $1 \times 10^{-5} \text{ g ml}^{-1}$  target protein IgG. Insets are the schematics of corresponding ZnO NW devices.

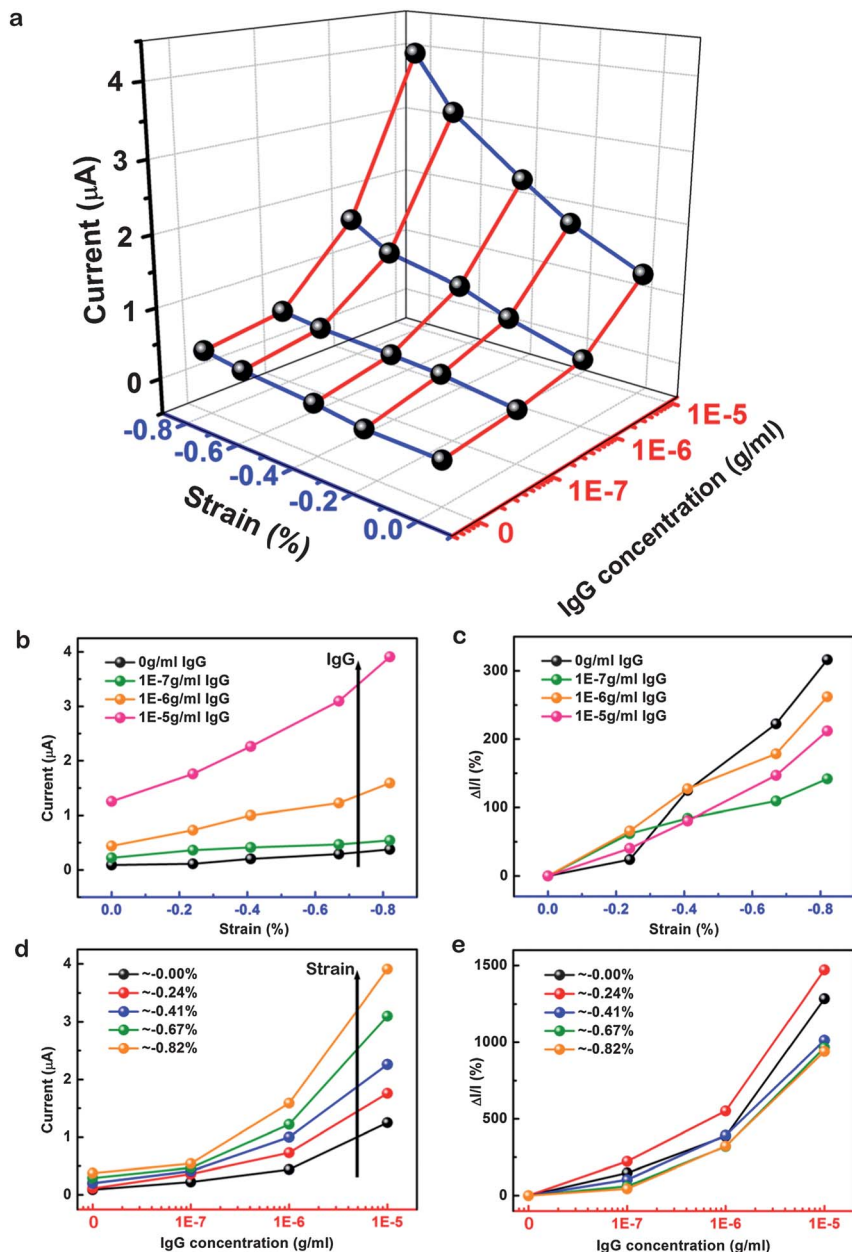


**Fig. 3** Piezotronic effect on the performance of ZnO NW protein sensors. (a) 3D graph depicting the current response of the ZnO NW protein sensor under different strains and IgG concentrations. (b and c) Absolute and relative current response of the ZnO NW protein sensor under different compressive strains, with the IgG concentration ranging from 0 to  $1 \times 10^{-5} \text{ g ml}^{-1}$ , respectively. (d and e) Absolute and relative current response of the ZnO NW protein sensor at different IgG concentrations, with compressive strain ranging from 0 to  $-0.82\%$ , respectively. Data of (b)–(e) were extracted from (a).

on increasing the strain, the difference between currents relative to two adjacent IgG concentrations was increased. That is to say, for example under strain 0% the difference between the current at  $1 \times 10^{-6} \text{ g ml}^{-1}$  IgG concentration and that at  $1 \times 10^{-5} \text{ g ml}^{-1}$  IgG concentration is around  $0.41 \mu\text{A}$ , while this difference under strain  $-0.82\%$  increases to  $2.3 \mu\text{A}$ , which is increased by more than 50 times. It means that the piezotronic effect largely enhanced the resolution of the protein sensors, which is the result of the non-linear  $I$ - $V$  transport properties as created by the Schottky barrier at the contacts of the M-S-M structure. Fig. 3d and e present the absolute and relative current response of the

ZnO NW protein sensor to different IgG concentrations, with compressive strain fixed in each curve, ranging from 0 to  $-0.82\%$ , respectively. These 2D graphs present five curves under five different externally applied compressive strains, each was derived by measuring the output current of the ZnO NW protein sensor at different IgG concentrations. Furthermore, it can be seen from this graph that at a fixed IgG concentration, the larger the strain the higher the output current: at a very low IgG concentration, without applying external strains, the output current might be too small to be detected, while applying a compressive strain, the output signal could be enhanced large



enough to be detected. That is to say, the piezotronic effect can improve the detection limit or sensitivity of ZnO NW protein sensors.

A theoretical model is proposed to explain the piezotronic effect on the performance of ZnO NW protein sensors using energy band diagrams, as shown in Fig. 4. The silver electrodes and the n-type ZnO NW form a contact; the energy barrier at the interface is relatively low since the work function of silver does not deviate from the electron affinity of ZnO NW significantly, as shown in Fig. 4a. Since the ZnO semiconducting NW also exhibits a piezoelectric effect, a strain in the structure would produce piezo-charges at the interfacial region. It is important to note that the polarization charges are distributed within a small depth from the surface, and they are ionic charges, which are non-mobile charges located adjacent to the interface. Under this circumstance, free carriers can only partially screen the piezo-charges instead of completely canceling out all of them. Thus a piezopotential is produced inside the NW. A positive piezopotential may effectively lower the barrier height at the local contact, while a negative piezopotential increases the barrier height. The role played by the piezopotential is to effectively change the local contact characteristics through an internal field depending on the crystallographic orientation of the material and the sign of the strain, thus the charge carrier transport process is tuned at the M–S contact.<sup>27,28</sup> This explains well the shape transformation of  $I$ – $V$  curves from “Ohmic type” to “Schottky type” under different compressive strains, as shown in Fig. 2.

Fig. 4b illustrates the working principle of a piezotronic transistor (*i.e.* ZnO NW protein sensors) using the band structure of the device. A strain free ZnO NW protein sensor has Ohmic-like contacts at the two ends with the source and drain electrodes, as presented in Fig. 4a. A piezopotential is created along the NW ( $c$ -axis) once it is subjected to mechanical straining, which reduces and increases the local barrier heights at the two ends, respectively, and transforms one of the contacts from Ohmic to Schottky type, which is a characteristic of the piezotronic effect. When the ZnO NW protein sensor is compressively strained, a positive piezopotential at the drain electrode lowered local SBH, while a negative piezopotential at the other side raised it up, as shown in Fig. 4b. Considering the asymmetric M–S–M structure with SBH at one M–S contact interface differing significantly from the other, it has been proved<sup>25</sup> that only the reversibly biased Schottky contact (*i.e.* the drain here) dominates the transport properties inside ZnO NW devices. Therefore, on increasing the externally applied compressive strain, the local SBH at the drain becomes lower, which leads to a higher transport current of the ZnO NW protein sensor.

Fig. 4c presents a schematic and the corresponding band structure of an anti-IgG surface functionalized ZnO NW device under compressive strain, binding with the target protein IgG. IgG is a molecule that consists of four peptide chains (two heavy chains and two light chains)<sup>20</sup> and the amine groups at the end of the chains are positively charged. Therefore, the attachment of a positively charged molecule, such as IgG, to the n-type ZnO NW

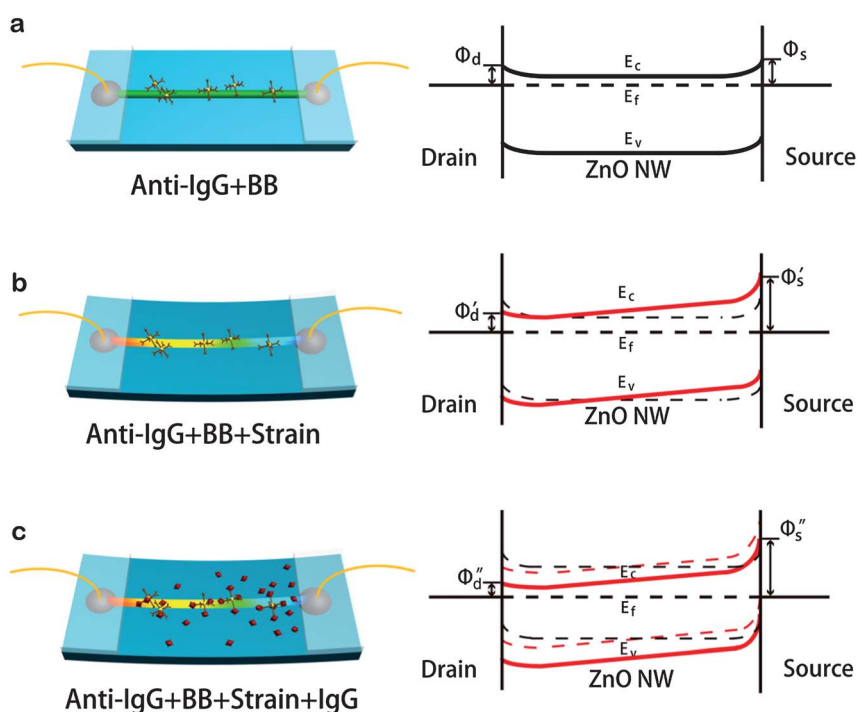


**Fig. 4** Schematic band structure of ZnO NW devices illustrating the asymmetric Schottky barriers at source and drain contacts of the ZnO NW protein sensor when it was (a) unstrained (presented as solid black lines in (a), dashed black lines in (b) and (c)), (b) compressively strained with the surface functionalized with anti-IgG and BB, but without binding the target protein IgG (presented as solid red lines in (b), dashed red lines in (c)), (c) compressively strained and surface functionalized with anti-IgG and BB, and binding with the target protein IgG (presented as solid red lines in (c)).

device is equivalent to a positive potential gating that leads to an increased electron density of the ZnO NW protein sensor.<sup>19</sup> Such a positive “gate” acts the same by lowering the conduction and valence bands of ZnO simultaneously, thus increasing the output current, as shown in Fig. 4c. Moreover, the target protein IgG may not be uniformly distributed along the surface of ZnO NW, the negative piezopotential side may have a higher IgG concentration because of the charge attraction, thus effectively lowering the local contact potential. These are the reasons why the higher the bonding IgG concentration, the higher the output signals of ZnO NW protein sensors, as observed in experiments.

Finally, we discuss about the stability of ZnO NWs in bio-solution. During the experiments, 0.005 ml IgG sample with a certain concentration was pipetted onto the ZnO NW device. Each time after adding the IgG sample onto the ZnO NW, the device was left to dry for one hour followed by measurements for another four to five hours. This process was repeated for five times with five different IgG concentrations. Typically, it took several days to finish the whole procedure of measuring one device. Our results show that the devices can perform stably during the whole experiment, which was several days long. Therefore, ZnO NWs can maintain their stability in bio-solution for a time period long enough for repeated measurements thousands of times in practical applications.

In summary, a M–S–M Schottky contacted ZnO NW device was introduced to work as an IgG-targeted protein sensor. By applying a compressive strain, the performance of the ZnO NW protein sensors was systematically studied. The piezotronic effect on the ZnO NW protein sensor can not only increase its resolution for protein sensing by tens of times, but also largely improve the detection limit and sensitivity. A theoretical model is proposed to explain the observed behaviors of the sensor. This study demonstrates an approach to raise the resolution, improve the detection limit and enhance the general performance of a biosensor.

## Acknowledgements

The research was supported by Airforce, MURI, U.S. Department of Energy, Office of Basic Energy Sciences (DE-FG02-07ER46394), NSF, and the Knowledge Innovation Program of the Chinese Academy of Sciences (KJXC2-YW-M13).

## Notes and references

- V. J. Higgins, P. J. Rogers and I. W. Dawes, *Appl. Environ. Microbiol.*, 2003, **69**, 7535–7540.
- K. K. Jain, *Clin. Chem.*, 2007, **53**, 2002–2009.
- S. M. Lee, S. B. Lee, C. H. Park and J. Choi, *Chemosphere*, 2006, **65**, 1074–1081.
- X. J. Duan, R. X. Gao, P. Xie, T. Cohen-Karni, Q. Qing, H. S. Choe, B. Z. Tian, X. C. Jiang and C. M. Lieber, *Nat. Nanotechnol.*, 2012, **7**, 174–179.
- B. Z. Tian, T. Cohen-Karni, Q. Qing, X. J. Duan, P. Xie and C. M. Lieber, *Science*, 2010, **329**, 830–834.
- K. Tomioka, M. Yoshimura and T. Fukui, *Nature*, 2012, **488**, 189–192.
- E. Stern, J. F. Klemic, D. A. Routenberg, P. N. Wyrembak, D. B. Turner-Evans, A. D. Hamilton, D. A. LaVan, T. M. Fahmy and M. A. Reed, *Nature*, 2007, **445**, 519–522.
- G. F. Zheng, F. Patolsky and C. M. Lieber, *Abstr. Pap. Am. Chem. Soc.*, 2005, **230**, U306–U307.
- G. F. Zheng, F. Patolsky, Y. Cui, W. U. Wang and C. M. Lieber, *Nat. Biotechnol.*, 2005, **23**, 1294–1301.
- X. X. Duan, Y. Li, N. K. Rajan, D. A. Routenberg, Y. Modis and M. A. Reed, *Nat. Nanotechnol.*, 2012, **7**, 401–407.
- Y. Cui, J. P. Barford and R. Renneberg, *Biotechnol. Lett.*, 2006, **28**, 1835–1840.
- Z. L. Wang, *Nano Today*, 2010, **5**, 540–552.
- Z. L. Wang, *Adv. Mater.*, 2012, **24**, 4630–4631.
- J. Zhou, Y. D. Gu, P. Fei, W. J. Mai, Y. F. Gao, R. S. Yang, G. Bao and Z. L. Wang, *Nano Lett.*, 2008, **8**, 3035–3040.
- A. K. Sood, E. J. Egerton, Y. R. Puri, J. Zeller, T. Manzur, D. L. Polla, N. K. Dhar, J. Zhou, S. Xu, S. Zhang, Z. L. Wang and A. F. M. Anwar, *Oxide-based Materials and Devices II*, 2011, p. 7940.
- Q. Yang, X. Guo, W. H. Wang, Y. Zhang, S. Xu, D. H. Lien and Z. L. Wang, *ACS Nano*, 2010, **4**, 6285–6291.
- Q. Yang, W. H. Wang, S. Xu and Z. L. Wang, *Nano Lett.*, 2011, **11**, 4012–4017.
- S. Mao, K. H. Yu, G. H. Lu and J. H. Chen, *Nano Res.*, 2011, **4**, 921–930.
- X. C. Dong, Y. M. Shi, W. Huang, P. Chen and L. J. Li, *Adv. Mater.*, 2010, **22**, 1649–1653.
- S. Mao, G. H. Lu, K. H. Yu, Z. Bo and J. H. Chen, *Adv. Mater.*, 2010, **22**, 3521–3526.
- Z. W. Pan, Z. R. Dai and Z. L. Wang, *Science*, 2001, **291**, 1947–1949.
- M. Eichenfield, J. Chan, R. M. Camacho, K. J. Vahala and O. Painter, *Nature*, 2009, **462**, 78–82.
- R. S. Yang, Y. Qin, L. M. Dai and Z. L. Wang, *Nat. Nanotechnol.*, 2009, **4**, 34–39.
- J. Zhou, P. Fei, Y. D. Gu, W. J. Mai, Y. F. Gao, R. Yang, G. Bao and Z. L. Wang, *Nano Lett.*, 2008, **8**, 3973–3977.
- R. M. Yu, L. Dong, C. F. Pan, S. M. Niu, H. F. Liu, W. Liu, S. Chua, D. Z. Chi and Z. L. Wang, *Adv. Mater.*, 2012, **24**, 3532–3537.
- C. F. Pan, Z. T. Li, W. X. Guo, J. Zhu and Z. L. Wang, *Angew. Chem., Int. Ed.*, 2011, **50**, 11192–11196.
- Z. L. Wang, *ACS Nano*, 2008, **2**, 1987–1992.
- Z. L. Wang, *MRS Bull.*, 2012, 814–827.